UC Davis

UC Davis Previously Published Works

Title

Fabrication, detection, and analysis of DNA-labeled PLGA particles for environmental transport studies

Permalink

https://escholarship.org/uc/item/0gf6h1s2

Authors

McNew, Coy P
Wang, Chaozi
Walter, M Todd
et al.

Publication Date

2018-09-01

DOI

10.1016/j.jcis.2018.04.059

Peer reviewed

eScholarship.org Powered by the California Digital Library
University of California

Accepted Manuscript

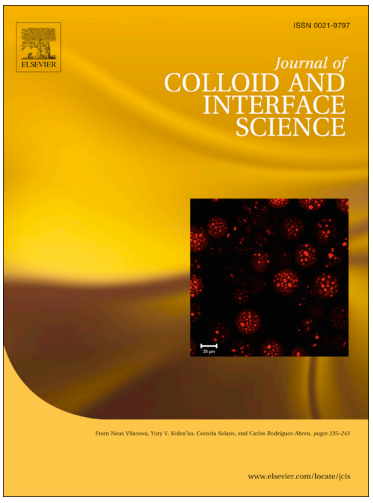

Fabrication, Detection, and Analysis of DNA-labeled PLGA Particles for Environmental Transport Studies

Coy P. McNew, Chaozi Wang, M. Todd Walter, Helen E. Dahlke

PII: S0021-9797(18)30446-6
DOI: https://doi.org/10.1016/j.jcis.2018.04.059
Reference: YJCIS 23524

To appear in: *Journal of Colloid and Interface Science*

Received Date: 27 October 2017
Accepted Date: 15 April 2018

Please cite this article as: C.P. McNew, C. Wang, M. Todd Walter, H.E. Dahlke, Fabrication, Detection, and Analysis of DNA-labeled PLGA Particles for Environmental Transport Studies, *Journal of Colloid and Interface Science* (2018), doi: https://doi.org/10.1016/j.jcis.2018.04.059

This is a PDF file of an unedited manuscript that has been accepted for publication. As a service to our customers we are providing this early version of the manuscript. The manuscript will undergo copyediting, typesetting, and review of the resulting proof before it is published in its final form. Please note that during the production process errors may be discovered which could affect the content, and all legal disclaimers that apply to the journal pertain.

ACCEPTED MANUSCRIPT

Fabrication, Detection, and Analysis of DNA-labeled PLGA Particles for Environmental Transport Studies

Coy P. McNew[a,*], Chaozi Wang[a], M. Todd Walter[b], Helen E. Dahlke[a]

[a] *Department of Land, Air, and Water Resources, University of California, Davis, Davis, CA 95616, USA*
[b] *Department of Biological and Environmental Engineering, Cornell University, Ithaca, NY 14853, USA*

Abstract

Poly(lactic-*co*-glycolic acid) (PLGA) particle carriers of synthetic DNA have recently received increased attention for environmental applications due to their biodegradability, customizability, and nearly limitless number of uniquely identifiable "labels". In this paper, we present methodologies for the preparation of DNA-labeled particles, control of particle size, extraction of DNA-labels, and analysis via quantitative polymerase chain reaction (qPCR). Characterization and analysis of the DNA-labeled particles reveal spherical particles of diameters ranging from 60 – 1,000 nm, with consistent zeta potentials around -45 mV, that are stable to aggregation, even in the presence of concentrated mono- and divalent cations. A highly correlated and consistent relationship between particle concentration and DNA-label count was observed, with a detection range spanning 7 orders of magnitude, from 0.01 - 10,000 mg/L (10 - 10^7 particles/μL). The results of two environmental applications of the DNA-labeled particles are also presented, highlighting their feasibility for use in environmental studies. Whether exploring size-dependent transport phenomena or identifying potential pathogen transport pathways, the DNA-labeled particle approach presented here provides a powerful tool for the identification of overlapping particle signals at a range of concentrations.

*Corresponding author
Email address: cpmcnew@ucdavis.edu (Coy P. McNew)

ACCEPTED MANUSCRIPT

Keywords: PLGA, DNA, colloid, transport

1. Introduction

Polymeric nano- and microparticles have garnered considerable attention in recent years for their many applications as colloidal carriers of drugs, DNA, and other macromolecules in the field of life sciences, biotechnology, and medical sciences [1, 2, 3]. Among the many polymeric nano- and microparticles developed to date, poly(lactic-*co*-glycolic acid) (PLGA) has become the most widely used polymer in FDA-approved pharmaceutical biotechnology and medical devices [4]. This is due to two of its most attractive qualities, biodegradability and non-toxicity, which provide key advantages for its use in oral delivery of proteins, peptides, and synthetic DNA for treatment of several life-threatening diseases [5]. PLGA provides a number of therapeutic benefits in drug delivery such as controlled particle size [6, 7], higher loading capacity for drug molecules [8], improved drug stability and bioavailability [9, 10], and controlled and sustained release properties [11, 12]. In comparison to nonbiodegradable, inorganic nanoparticles (e.g. metallic, silica or carbon-based nanomaterials), which are often used in the cosmetic and paint industry, PLGA nano- and microparticles also do not represent a risk to the aquatic environment, since their biodegradability limits their persistence in the environment [13].

Because of their versatility, PLGA particles carrying synthetic DNA strands have received increasing attention over the past 15 years, for use in environmental applications such as the identification and characterization of water flow and pollutant transport pathways [13, 14, 15, 16]. The use of synthetic DNA provides virtually an infinite number of unique labels (i.e. tracers) while the customizable PLGA nano- and microspheres protect the DNA from the environment. Hence, a multitude of unique, DNA-labeled particle tracers could be introduced at different points and times in the landscape, for example a watershed characterized by non-point source pollution, and collected in water samples elsewhere in the watershed to infer hydrological linkages and transport times between the

ACCEPTED MANUSCRIPT

collection point(s) and the points of DNA introduction. As such, DNA-labeled PLGA particles provide a new tracer technology for hydrologic and environmental sciences and a means for overcoming some of the obvious challenges of conventional, conservative tracers [14].

Various techniques have been explored to encapsulate macromolecules with PLGA, two of the most common techniques for the encapsulation of hydrophilic macromolecules are double emulsion evaporation ($w_1/o/w_2$) and nanoprecipitation [1]. Among the hydrophilic macromolecules explored, several studies have developed PLGA carriers for DNA [17, 18, 19] intended for gene therapy within the human body. By instead incorporating synthetic DNA within the PLGA, any number of unique particle tracers can be fabricated with DNA-"labels" (i.e. a unique nucleotide sequence), which can then be independently detected and quantified via quantitative polymerase chain reaction (qPCR) [13]. Additionally, any PLGA released to the environment will degrade and the degree of biodegradability can be altered through modification of the polymer, providing biodegradability on the order of weeks, months, or years [11, 12] and the ability to match its environmental lifespan with the length of an environmental study. Together these characteristics provide many advantages over conventional particle and hydrologic tracers. Historically, a variety of tracers have been used to identify and characterize environmental transport pathways, including bromide [20, 21], chloride [22, 23], nano- and microparticles [24, 25, 26], dyes [27, 28], and isotopes [29, 30]. However each of these methods is limited in one or more ways. Most importantly, the number of unique tracers available is limited [14, 31], hence our ability to identify spatial and temporal variations is restricted to only a few events [32], leaving us far short of the information needed to understand the complex transport pathways in the natural environment. Furthermore, contamination from legacy tracers left over from past experiments [33, 34] can alter transport measurements and often it is difficult to determine just how long a system may retain a "memory" of past inputs. Ultimately, a tracer system that allows for the unique identification between spatial, temporal, and variable particle characteristic (i.e. size) inputs with otherwise identical colloidal prop-

ACCEPTED MANUSCRIPT

erties, would allow for a much more powerful characterization, description, and, ultimately, prediction of transport pathways in the environment.

The use of unencapsulated, synthetic DNA as an environmental tracer has previously been explored [35, 36] and, although it has proven useful in identifying contaminant source contributions in limited cases [36, 37], DNA has the disadvantage of degrading quickly in the natural environment, unless bound to natural colloids [38] or polycyclic aromatic hydrocarbons. In order to control the degradation of the synthetic DNA sequences and allow for quantitative experiments at time scales required for field studies, we previously explored encapsulating DNA in poly lactic acid (PLA) microspheres in a proof-of-concept study [13] and then applied this technology to characterize hydrologic flow pathways through a 3.2 km^2 glacier in northern Sweden [14]. In the study by Dahlke et al.[14], nine unique DNA-labeled tracers were applied at spatially varying locations throughout the glacier and breakthroughs were monitored. Though mass recovery of the DNA-labeled tracers was lower than that of fluorescent dye, advection-dispersion information obtained from the tracers provided insight into the complex hydrologic flow pathway system of the glacier.

In this paper, we present new advances in DNA-labeled particle tracer technology for use in environmental and hydrological flow and transport studies. Detailed methodologies are introduced for the preparation of DNA-labeled particles, control of particle size, extraction of synthetic DNA-labels, and quantitative analysis via qPCR. An in depth characterization of particle properties is also provided, including particle morphology, size, charge, colloidal stability, and encapsulation and extraction efficiencies. Furthermore, the relationship between particle mass concentration and DNA-label count is analyzed, which is an important aspect for using the DNA-labeled particles in quantitative fate and transport studies. Finally, we present the results from two environmental applications of the DNA-labeled particles, which highlight their feasibility for use in environmental studies.

ACCEPTED MANUSCRIPT

2. Experimental

2.1. Materials

Research grade 50:50 poly(DL-lactide-*co*-glycolide) (PLGA) was purchased from LACTEL Absorbable Polymers (B6010-2, Birmingham, AL). HPLC grade ethyl acetate (EtAc, E195), dichloromethane 99+% (DCM, L13089), reagent grade ethyl alcohol (AX0441), and 50X molecular biology grade tris-EDTA (TE) buffer (75834) were purchased from Fisher Scientific. Vitamin E-D-α-tocopherol polyethylene glycol succinate (TPGS, 57668) and reagent grade dimethyl sulfoxide (DMSO, 472301) were purchased from Sigma-Aldrich.

SsoAdvanced ™Universal SYBR ®Green Supermix (172-5271) and SsoAdvanced™ Universal Probes Supermix (172-5281) were purchased from Bio-Rad Laboratories, Inc. All synthetic, double-stranded DNA sequences used for particle labeling, primers, and probes for qPCR analysis were purchased from Integrated DNA Technologies (IDT Inc., Coralville, Iowa, USA). All sequences, primers, and probes used in this study are listed in Table B.1.

2.2. Particle Fabrication

The DNA-labeled particles were fabricated by dispersing synthetic DNA in a PLGA/solvent mixture, which was then dispersed into an aqueous phase by one of two methods: $w_1/o/w_2$ emulsion evaporation or nanoprecipitation. After hardening the particles, they were collected through centrifugation and rinsed in ultrapure DI water to remove the unbound surfactant used in the process, along with any unincorporated DNA-labels. Through variations in surfactant concentration ($w_1/o/w_2$ emulsion evaporation method) and injection type (nanoprecipitation method), the size of the resultant particles was controlled.

2.2.1. Double emulsion ($w_1/o/w_2$) method

The $w_1/o/w_2$ fabrication method employed is similar to the methods previously presented in literature [39, 1] with some modifications described as follows. First, 100 mg PLGA was mixed with 1 mL EtAc in a test tube and left to dissolve overnight. The next morning, 45 mL of the TPGS solution of desired

ACCEPTED MANUSCRIPT

concentration was added to a 250 mL beaker on a magnetic stir plate and 2 mL was added to a test tube. 25 μL of the desired DNA-label (4×10^{-6}M) was added to the PLGA/EtAc mixture and sonicated (Branson Ultransonics SLPe Digital Sonifier, 40% amplitude, 1/8" diameter tip) for 10 seconds, on ice, to make the first emulsion. This emulsion is then added dropwise to the 2 mL of TPGS, while constantly vortexing at 3,000 rpm, to make the second emulsion. The second emulsion was then sonicated for three 10 second bursts, on ice, with a 10 second rest after each burst. This final emulsion was then added to the stirring 45 mL of TPGS solution and left to stir in a fume hood for at least 4 hours or overnight. During this time, the EtAc evaporated, hardening the PLGA particles.

2.2.2. Nanoprecipitation

The nanoprecipitation method employed is similar to methods previously presented in literature [17, 40, 41] with some modifications described as follows. First, 20 mg PLGA was mixed with 1 mL DMSO in a test tube and left to dissolve overnight. The next morning, 20 mL 0.3% (w/v) TPGS was added to a 50 mL beaker on a magnetic stir plate. 5 μL of the desired DNA-label (4×10^{-6}M) was added to the PLGA/DMSO mixture and sonicated (40% amplitude, 1/8" diameter tip) for 10 seconds, on ice. This mixture was then added to the stirring beaker of TPGS solution at 30 mL/hr by a syringe pump (New Era Pump Systems NE-1000) with the syringe tip either above (indirect) or below (direct) the surface of the stirring liquid. This emulsion was then left to stir in a fume hood for at least 4 hours or overnight, during which time the DMSO evaporated, hardening the PLGA particles.

To collect and rinse the particles fabricated by either method, the particle suspension was poured into a 50 mL HDPE centrifuge tube, topped up to 50 mL total volume with ultrapure DI water (ELGA LabWater GS120A24) and centrifuged (Eppendorf 5804 R) at 14,600 x g at 4^oC for 15 minutes. After centrifugation, the supernatant was carefully removed so as not to disturb the particle pellet, and the particles were resuspended in ultrapure DI water by

ACCEPTED MANUSCRIPT

sonicating (40% amplitude, 1/8" tip) for three 10 second bursts on ice, with a 10 second rest after each burst. This centrifugation, rinsing, and resuspension step was repeated twice more, for a total of three times and then the stock particle suspension was stored at 2^{o}C until use.

2.2.3. Bare particles

As a basis for comparison, bare PLGA particles were fabricated in the absence of TPGS, as macromolecules similar to TPGS have been shown to adsorb to the surface of the PLGA particles, altering their colloidal properties [42, 43, 44]. The method used to prepare the bare PLGA particles was similar to others previously presented [43, 42, 1] and explained in detail in Appendix A.

2.3. Particle quantification

2.3.1. DNA-label extraction

The procedure for the analysis of DNA-labeled particle samples consists of two steps, extraction and quantification of the DNA-labels. First, a well-mixed 500 μL aliquot of each sample was collected in a 1.5 mL centrifuge tube, centrifuged at 14,600 x g, 4^{o}C for 15 minutes, and frozen at -80^{o}C for several hours. Each sample was then lyophilized, 500 μL DCM was added to the dry sample, and the resulting mixture was vortexed at 3,000 rpm for 10 seconds, to allow for dissolution of the PLGA. 500 μL of TE buffer solution (10 mM Tris, 1 mM EDTA, pH 8.0) was added to each sample and vortexed at 3,000 rpm for 30 seconds. The resulting two-phase liquid was then centrifuged at 2,800 x g, 4^{o}C for 5 minutes and 200 μL of the supernatant was removed for quantification.

2.3.2. DNA-label quantification

Quantification of the extracted DNA-labels was performed with real-time, quantitative polymerase chain reaction (qPCR, Bio-Rad CFX96 Touch), in 10 μL total volume wells. Two reaction methods were used, single-channel for the analysis of one type of DNA-label at a time, and multi-channel for the

ACCEPTED MANUSCRIPT

simultaneous analysis of up to six DNA sequences at a time (depends on the qPCR multiplexing capability). The single-channel reactions consisted of 5 μL SsoAdvanced ™Universal SYBR ®Green Supermix, 4 μL sample, 0.4 μL each forward and reverse primer (resulting in a final primer concentration of 1 μM each), and 0.2 μL nuclease-free water. The multi-channel reactions consisted of 5 μL SsoAdvanced ™Universal Probes Supermix, 4 μL sample, and 1 μL total of the forward primer, reverse primer, and Taqman probe for each DNA-label to be analyzed, resulting in final concentrations of 0.4 μM, 0.4 μM, and 0.2 μM, respectively. In order to determine the number of DNA molecules present in each sample, standards of known concentration were included on each plate and a standard curve was produced to relate the quantification cycle (C_q) value to DNA copy count. The upper and lower DNA detection limits are then defined by the portion of the standard curve where the C_q and DNA copy count correlate with an $R^2 \geq 0.99$. Though slight variations occur for each DNA sequence, this detection range typically falls between 100 and 10^8 copies per sample, or 25 to 2.5 x 10^7 copies/μL. In this manner, the DNA copy count was always interpolated from standards included on each plate and never extrapolated. A representative standard curve can be seen in Figure 1 for the nucleotide sequence T3, which was used for all experiments in this study, unless otherwise noted. The resultant detection range for this sequence was 150 to 10^7 copies per 4 μL sample, or 38 - 2.5 x 10^6 copies/μL. The C_q value for each sample was calculated with the Bio-Rad software (Bio-Rad CFX Manager 3.1) using the regression C_q determination mode with baseline subtracted curve fit. Each sample was analyzed in triplicate to provide statistical uncertainty of the measurement.

It should be noted here that the presence of natural organic matter can affect the fluorescence measured by qPCR and therefore the reported DNA count. By preparing all standards in water containing identical organic content to the collected samples, this background effect can be subtracted, providing true DNA counts. This can be easily achieved by collecting water samples before the introduction of any DNA-labeled particles to prepare all standards

ACCEPTED MANUSCRIPT

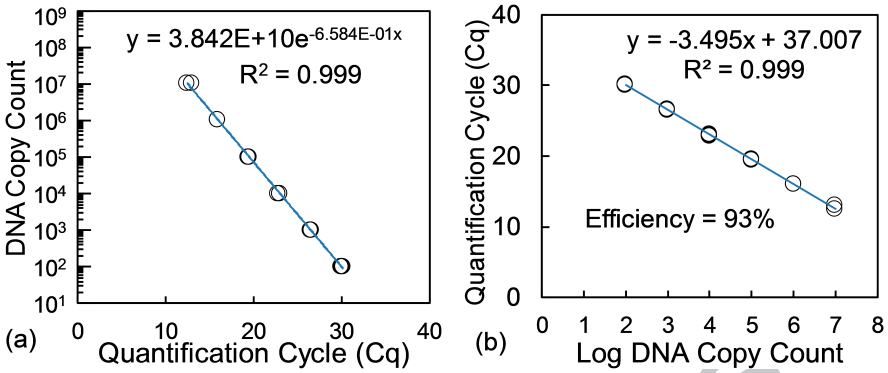

Figure 1: Representative qPCR standard curve for the quantification of the T3 DNA sequence (a) and calculation of the qPCR replication efficiency (b). Each measurement was performed in triplicate and the resultant detection range for this sequence was 150 - 10^7 copies per 4 μL sample.

needed for the qPCR analysis of the experiment.

2.4. DNA-label design

The synthetic, double-stranded DNA sequences used for particle labeling were designed as described in our previous publications [13, 14]. A list of the nucleotide sequences, primers, and probes used for this study can be found in Table B.1. For both qPCR reaction methods (e.g. single and multi-channel) forward and reverse primers are needed for each sequence. The multi-channel reaction method requires the use of a TaqMan probe, which consists of an additional short (5' to 3') sequence with a quencher on the 5' (e.g. ZEN internal quencher, Integrated DNA Technologies) and 3' (Iowa Black®forward quencher) end and a reporter dye such as TET (Dual-Labeled tetrachlorofluorescein), FAM (6-carboxyfluorescein amidite), or HEX (hexachlorofluorescein). It should also be noted here that during the design of each sequence, the National Center for Biotechnology Information's Nucleotide Primer-BLAST Tool [45] is used to ensure that the selected sequences have no similarities to natural DNA.

ACCEPTED MANUSCRIPT

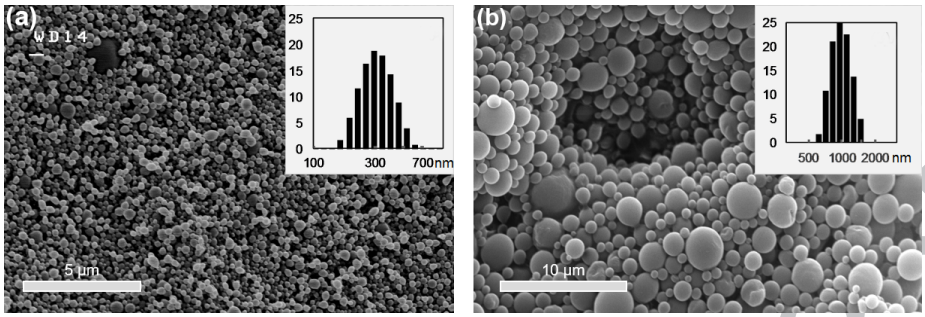

Figure 2: Representative SEM images and particle diameter distributions of DNA-labeled particles fabricated via the $w_1/o/w_2$ method with (a) 0.30% TPGS and (b) 0.05% TPGS

3. Results and Discussion

3.1. Particle Characterization

Particle morphology was investigated using Field Emission Scanning Electron Microscopy images (FE-SEM, Hitachi S-4100T, Hitachi HTA America, with an Oxford INCA Energy EDS). Representative FE-SEM images of DNA-labeled particles with corresponding particle size distributions can be seen in Figure 2. The particles appear mostly spherical in nature with a small variation in particle diameter, as evidenced by the corresponding particle size distributions.

Particle diameter and zeta potential were measured using dynamic light scattering (DLS, Malvern Zetasizer Nano). Each reported value is a summary of at least 10 independent measurements, particle size measurements were buffered to pH 7 with TE (10 mM Tris, 1 mM EDTA), and particle concentration was held constant at 100 mg/L (2.8×10^5 particles/μL). A summary of the mean particle diameter and zeta potential for 6 different particle preparation conditions can be seen in Figure 3 and tabulated data can be found in Table D.9.

Particle diameter varied between 60 and 930 nm for the particle preparation conditions investigated, with the smallest particles produced via the nanoprecipitation method. Particle diameter was strongly dependent upon TPGS concentration, with smaller particles resulting from higher TPGS concentrations,

ACCEPTED MANUSCRIPT

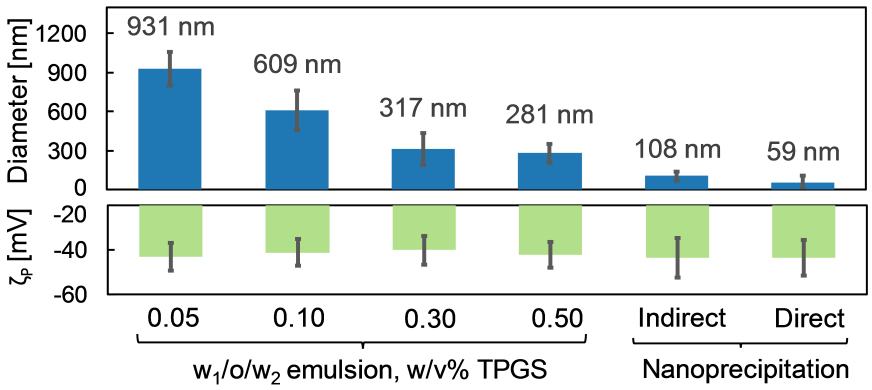

Figure 3: Summary of mean particle diameter and mean zeta potential of DNA-labeled particles for 6 different preparation conditions. Each reported value consists of at least 10 independent measurements, error bars represent standard deviation, and pH was held constant at 7.

as expected [39, 1]. Despite strongly affecting particle diameter, the preparation conditions had no detectable effect on zeta potential.

While it is unlikely that the preparation of subsequent batches under the same conditions will produce particles of identical diameter and zeta potential, we have found that the reproducibility between batches is quite consistent. For example, subsequent batches prepared using the $w_1/o/w_2$ method with 0.30% TPGS produced particles with mean diameters of 315, 323, 314, 321 nm, corresponding standard deviations of 117, 116, 102, 101 nm, and mean zeta potentials of -43, -44, -41, -40 mV.

The electrophoretic mobility (μ_e) and zeta potential of bare and DNA-labeled particles was measured as a function of solution pH and a summary of the data can be seen in Figure 4. Both bare and DNA-labeled particles remain negatively charged throughout the pH range investigated (pH 3 - 9), with declining charge as pH conditions became more acidic, suggesting an isoelectric point near or below pH 3. The DNA-labeled particles displayed a lower (absolute value) charge than the bare particles, with the largest differences observed

ACCEPTED MANUSCRIPT

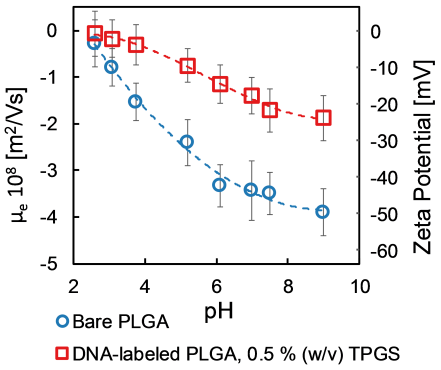

Figure 4: Electrophoretic mobility (μ_e) and zeta potential of bare PLGA and DNA-labeled particles as a function of pH. Error bars represent standard deviation.

near pH 7-8. This suggests that the TPGS, used in particle preparation as an emulsifier, remains bound to the particle surface after the rinsing and centrifugation step of particle preparation. While the hydrophobic end remains bound to the particle surface, the hydrophilic end extends into the aqueous medium, shifting the shear plane further from the particle surface and effectively lowering the electrophoretic mobility. Similar behavior has been reported for PLGA particles coated with other macromolecules [42, 43, 44].

3.1.1. Particle stability and aggregation

Time resolved DLS experiments were performed to characterize the stability of the bare and DNA-labeled particles in the presence of varying concentrations of NaCl and $CaCl_2$. As expected, aggregation rate increased with salt concentration for the bare PLGA particles (Figure C.11) with an increased sensitivity to the presence of divalent $CaCl_2$. Initial aggregation rates were constant throughout all salt concentrations investigated, and so the first 10 minutes of particle aggregation were used to calculate the critical coagulation concentration (CCC) in the presence of each salt. Details for the determination of the CCC and inverse stability factors (1/W) can be found in Appendix C. The results of this analysis are presented in Figure 5. In this manner, we determined the CCC values of bare PLGA particles to be 273 mM NaCl and 30 mM $CaCl_2$, which

ACCEPTED MANUSCRIPT

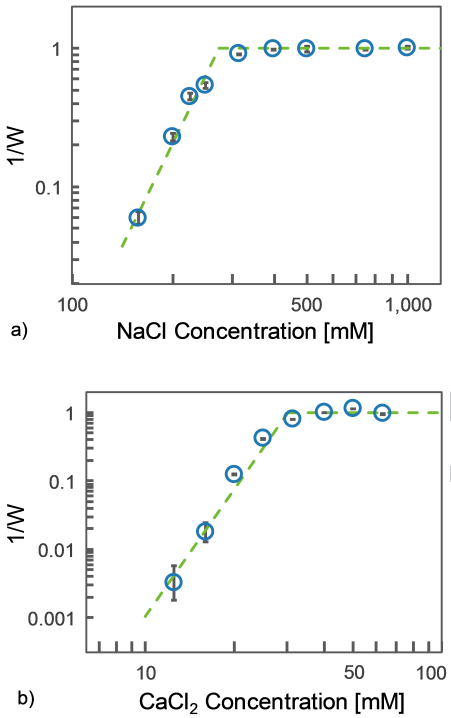

Figure 5: Inverse stability factor (1/W) of bare PLGA particles as a function of (a) NaCl and (b) $CaCl_2$ concentration. Error bars represent standard deviation. All experiments took place at pH 7 and particle concentration of 10 mg/L (2.8×10^4 particles/μL).

are similar to values reported in the literature [42, 43].

In contrast to the bare PLGA particles, DNA-labeled particles produced in the presence of TPGS showed no signs of particle aggregation across the full range of NaCl and $CaCl_2$ concentrations investigated for bare PLGA. Figure 6 displays the consistent particle diameters observed for DNA-labeled particles produced following several different preparation conditions, in the presence of 350 mM $CaCl_2$, which is an order of magnitude more concentrated that the CCC determined for bare PLGA particles (Figure 5).

This apparent stabilizing effect suggests that the TPGS not only serves as a high efficiency emulsifier and tool for controlled particle size [46] and increased encapsulation efficiency [47], but also remains adsorbed to the particle

ACCEPTED MANUSCRIPT

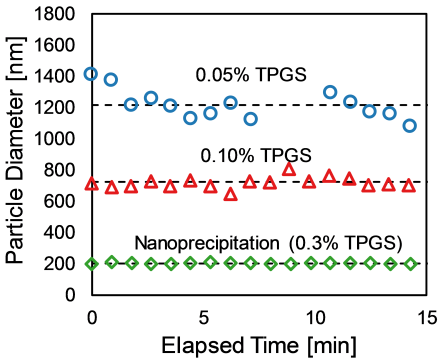

Figure 6: DNA-labeled particle diameter in the presence of 350 mM $CaCl_2$. All experiments took place at pH 7 and particle concentration of 10 mg/L (2.8×10^4 particles/μL).

surface after production and rinsing, increasing hydrophilicity of the particle and providing stabilization to aggregation. Similar stabilization behavior has been reported for other macromolecules including polaxamers and poloxamines [42, 43, 44], poly(ethylene glycol) (PEG) [48], and methoxy poly(ethylene glycol) (mPEG) [49, 50]. This stability enhancement resulting from macromolecule adsorption is commonly attributed to electrosteric repulsion, though a recent study by Bradford et al. [51] found that nanoscale roughness could also explain this behavior. This result is a key advantage for use in environmental systems where the ionic content of natural waters can lead to aggregation and therefore modified transport characteristics.

It should also be noted here that the particle diameters observed in the presence of concentrated $CaCl_2$ (Figure 6) were marginally higher than those in the absence of divalent cations (Figure 3), suggesting an initial period of rapid aggregation followed by consistent particle diameters throughout the length of experiments investigated in each case. Though the exact mechanism for this behavior is unclear, it has previously been observed for similar systems and detailed discussions can be found elsewhere [42].

ACCEPTED MANUSCRIPT

3.2. DNA-label Encapsulation and Extraction

In order to quantify the amount of DNA-labels encapsulated and to ensure consistency between preparation methods and batches, two measures of efficiency were defined and monitored. First, the percentage of DNA-labels that were successfully captured within the PLGA particles, commonly referred to as encapsulation efficiency (ENE), was determined from Equation 1, where DNA_{tot} is the total number of DNA copies used in particle preparation and DNA_{free} is the total number of unencapsulated DNA copies, determined from the supernatant following particle rinsing and centrifugation.

$$ENE = \frac{DNA_{tot} - DNA_{free}}{DNA_{tot}} \times 100\% \tag{1}$$

Second, the percentage of encapsulated DNA-labels that were subsequently extracted and counted, referred to here as the extraction efficiency (EXE), was determined from Equation 2, where DNA_{ext} is the total number of DNA copies extracted from the DNA-labeled particles and DNA_{encap} is the total number of DNA copies encapsulated within the DNA-labeled particles, determined from the encapsulation efficiency (Equation 1).

$$EXE = \frac{DNA_{ext}}{DNA_{encap}} \times 100\% \tag{2}$$

Encapsulation and extraction efficiency were calculated for several different particle preparation procedures described above (Figure 7). DNA-label encapsulation efficiency varied between 80 and 90% throughout the preparation methods explored. This is on the high end of literature reported values for the encapsulation of various drugs within PLGA particles, which range from 10% [52, 53, 54, 55, 56, 57, 58, 59] to 90% [60, 61, 62, 63, 64]. The high encapsulation efficiency values observed here are likely due to the properties of the emulsifier (TPGS) and DNA-labels themselves, as encapsulation efficiency is known to depend heavily on these factors [39, 64, 1] and TPGS has been reported to improve efficiency of emulsification and encapsulation [39, 46, 47].

ACCEPTED MANUSCRIPT

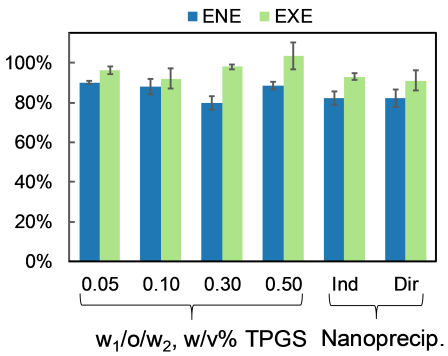

Figure 7: DNA-label encapsulation and extraction efficiency for various particle preparation methods. Error bars represent standard deviation.

DNA-label extraction efficiency varied between 90 and 100% throughout the preparation methods explored in Figure 7. Since the DNA-labeled particles are intended to be used as a tool to explore complex particle transport and hydrological experiments in the lab and environment, it is important that the particle detection, and therefore extraction efficiency, remain consistently at or near 100%, so the extraction efficiency values reported here provide confidence in the efficacy of the DNA-labeled particles for their intended use. As the intended application is quite novel, we are unaware of any reported values to compare with the values observed here. In order to further quantify the reliability and consistency of DNA-labeled particle detection, the extracted DNA-label concentration was measured over a wide range of particle concentrations (Figure 8).

The data included in Figure 8 represent the range of particle concentrations that produced a linear relationship between particle concentration and DNA-label copy count with an $R^2 \geq 0.99$. The highly correlated relationship suggests that the DNA-label count provides an accurate measure of particle concentration across a range of 7 orders of magnitude, from 0.01 mg/L to 10,000 mg/L (10 - 10^7 particles/μL). As mentioned earlier, in order for the DNA-labeled particle technology to be used as a transport measurement tool, a consistent

ACCEPTED MANUSCRIPT

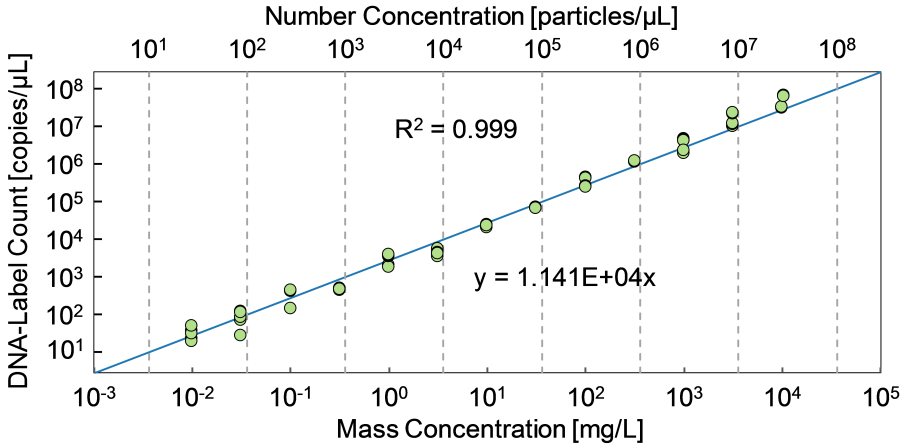

Figure 8: Summary of the relationship between DNA-labeled particle concentration and the extracted DNA count, as measured by qPCR.

relationship must be demonstrated between the DNA-label copy count and particle concentration. The nature of the relationship presented here suggests that particle detection by DNA-label quantification is consistent and reliable across a wide range of particle concentrations. It should also be mentioned here, that for the particles used in this particular analysis (800 nm diameter), the relationship between number concentration and DNA-label count resulted in a ratio of 1.2 DNA-labels per particle, on average. This ratio can be altered by varying the initial amount of DNA-labels used in particle preparation, and in turn, the range of detectable particle concentrations would shift in the same direction.

3.3. Environmental Applications

The main utility of the DNA-labeled particles lie in their ability to be used for environmental transport studies, therefore determining their performance under environmentally relevant conditions is of utmost importance. In this section we present the preliminary results from two ongoing studies as a proof-of-concept for the feasibility of environmental applications for the DNA-labeled particles. The first study investigates the subsurface lateral breakthrough of

ACCEPTED MANUSCRIPT

3 uniquely DNA-labeled particle applications through a small hillslope at the Sierra Foothills Research and Extension Center (SFREC) in Yuba County, CA. The second study investigates the long term stability and biodegradation of the DNA-labeled particles under various environmentally relevant conditions, including natural stream water sampled from two locations along Putah Creek, a tributary of the Sacramento River.

In order to test the suitability of the DNA-labeled particles for environmental field studies and evaluate our ability to distinguish between unique DNA-labeled signals in environmental samples, a subsurface lateral breakthrough experiment was conducted on a small hillslope at the SFREC facility in Yuba County, CA. The hillslope contains a vertically excavated trench face equipped with a water collection system, allowing for the sampling of subsurface lateral flow from each soil layer. The soil characteristics of the site have been evaluated in detail by Swarowsky et al. [65]. During experiments water was collected from three soil horizons, which included the A (0 - 10 cm), AB (10 - 25 cm), and Bt1 (25 - 65 cm) horizons of the Haploxeralfs soils at the site [65].

Two separate experiments were conducted on January 20, 2017 (Experiment 1) and February 21, 2017 (Experiment 2) at the hillslope, which varied greatly in rainfall amount, antecedent soil moisture content, and depth to perched water table. The soil depth-dependent breakthrough curves for Experiments 1 and 2 are presented in Figure 9. Due to the significant precipitation before and during Experiment 1, the hillslope formed a perched water table that reached the soil surface and signs of overland flow were observed during the event. One DNA-labeled particle tracer (10^{12} copy count; 309 $\pm$ 76 nm; T4 sequence) was applied 3 m upslope from the sampling point (i.e. trench face). Experiment 2 was conducted under drier conditions, with less precipitation before and during the experiment, resulting in a lower water table and no signs of overland flow. Two DNA-labeled particles tracers were simultaneously applied at 3 m (10^{12} copy count; 307 $\pm$ 70 nm; T10 sequence) and 5 m (10^{12} copy count; 309 $\pm$ 68 nm; T12 sequence) upslope from the sampling point.

Most importantly, both experiments resulted in breakthrough peaks at least

ACCEPTED MANUSCRIPT

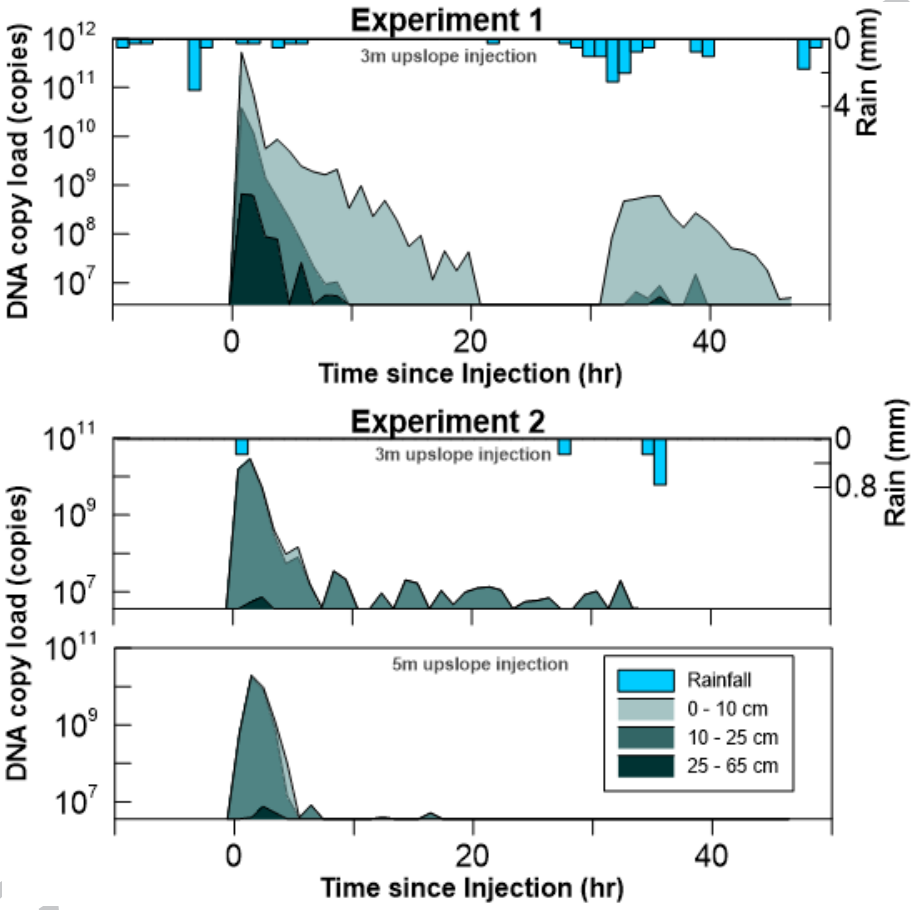

Figure 9: Soil-depth dependent breakthrough curves for Experiments 1 & 2, with corresponding 15 minute rainfall intensity.

ACCEPTED MANUSCRIPT

4 orders of magnitude above the detection limit and no difficulties were encountered distinguishing the DNA-labeled particles from background environmental DNA. Furthermore, each unique DNA-label in Experiment 2 was quantified independently, without interference from the other unique DNA-label applied simultaneously or from legacy DNA left over from Experiment 1. Interestingly, the particles were transported primarily in the top soil layer (0 - 10 cm) in Experiment 1, due to the high water table, with two breakthrough peaks corresponding to the two rainfall events. In Experiment 2, the particles were transported primarily in the second soil layer (10 - 25 cm), due to the lower water table. The results from these two experiments clearly provide evidence for the utility of DNA-labeled particle tracers for environmental applications, with no interference between unique DNA labels nor from background environmental DNA.

In order to determine the appropriate time scale for environmental applications and environmental stability of the DNA-labeled particles, a long-term degradation study was conducted. DNA-labeled particles (303 $\pm$ 72 nm, 100 mg/L) were prepared in DI water, NaCl (0.2 and 5.1 mM), and two different stream water samples. Stream water (SW) was sampled from two locations along Putah Creek, a tributary of the Sacramento River. SW 1 was sampled from a stagnant and turbid portion of the creek located on the UC Davis campus in Davis, CA and SW 2 was sampled from a fast moving and clear portion of the creek located upstream in Winters, CA. Additionally, each sample was held at two different temperatures (2 and 20 ^{o}C) for the entirety of the study. DNA-label concentration was then monitored over time and the results from the first 223 days are summarized in Figure 10.

While the DNA-label concentration remains relatively constant on the order of 10 days, a steady decline is observed after this point for all environmental conditions investigated. Most notably temperature appears to play a major role in the degradation rate. In each case, higher temperature results in an increased rate of degradation. NaCl appears to have no significant effect on degradation, as the degradation curves in the presence of NaCl appear very similar to those

ACCEPTED MANUSCRIPT

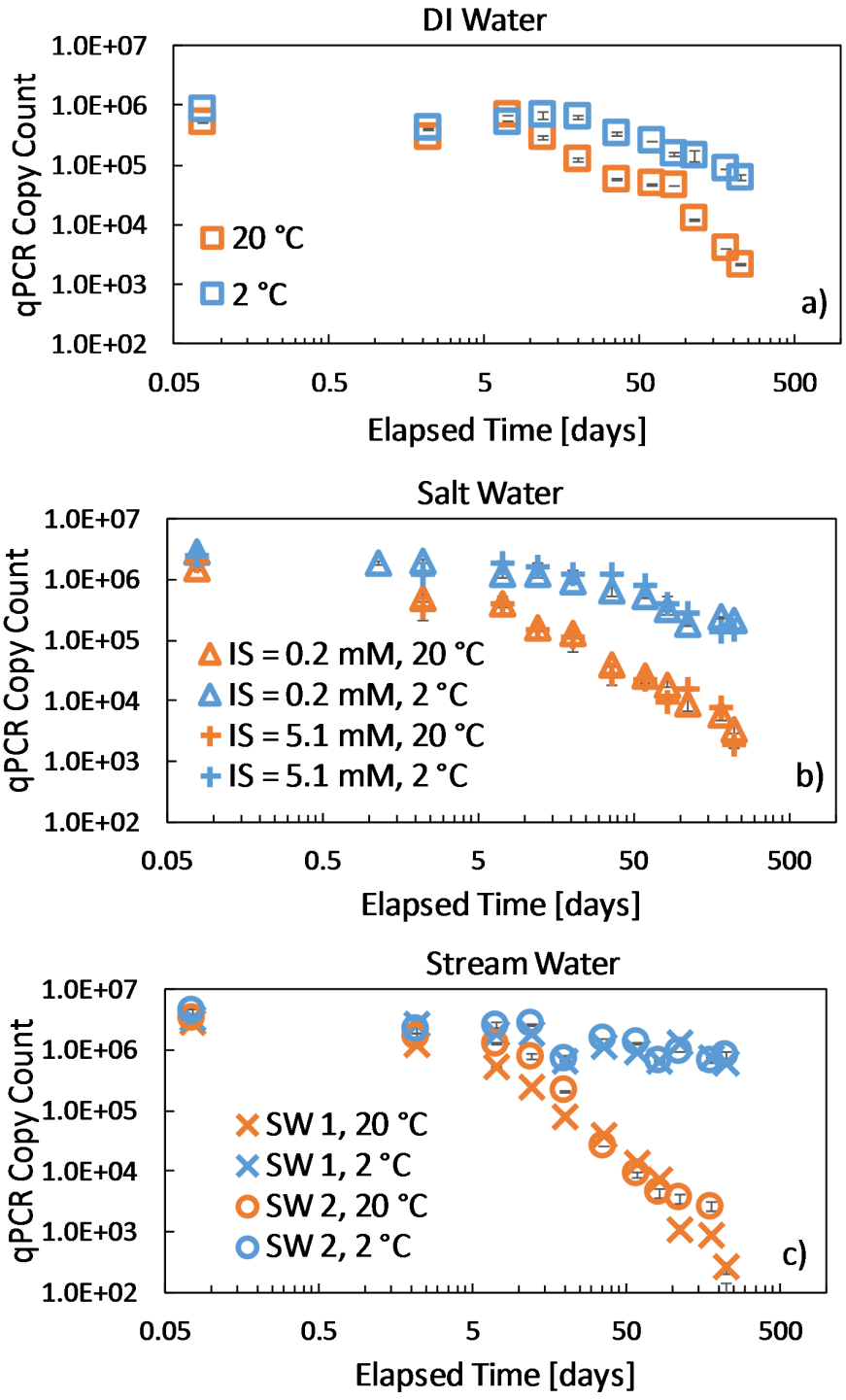

Figure 10: DNA-labeled particle degradation in the presence of DI water (a), NaCl (b), and stream water (c). Error bars represent standard deviation.

ACCEPTED MANUSCRIPT

in DI water. Interestingly, the presence of stream water appears to accelerate the degradation rate at 20 ^{o}C, while decreasing the degradation rate at 2 ^{o}C, as compared to DI water, and this effect was observed for both types of stream water. We would expect natural stream water to contain copious amounts of microbial life, leading to an increased rate of degradation, though the reason for the relatively flat trend at 2 ^{o}C is unclear.

After 223 days, DNA-label concentrations under all conditions investigated remain, at worst, an order of magnitude above the detection limit, with some remaining as high as 4 orders magnitude above the detection limit. These results are in general agreement with previously reported results on the biodegradability of similar PLGA particles, which are on the order of weeks to months [13, 11]. Biodegradability on this scale is ideal, as it ensures the DNA-labeled particles last long enough for experimental analysis, but don't persist to pollute the environment or contaminate future experiments with legacy DNA. Furthermore, these results reinforce the importance of control samples which are held at identical experimental conditions to account for degradation, as mentioned previously, especially for experiments lasting longer than 10 days.

4. Conclusions

Building from our previous work [13, 14, 15, 16], this study presents a comprehensive and detailed approach to the preparation, characterization, analysis, and quantitative detection of the DNA-labeled particle technology, a potentially powerful tool to study environmental flow and transport. While previous studies have demonstrated the utility of DNA [35, 36, 37] and DNA-labeled particles [13, 14, 15, 16] as environmental tracers, the current study reports advancements in the technology in several key areas, including size control, particle stability, and improved quantification. The introduction of TPGS into the particle preparation process produced particles stable to aggregation, even in the presence of concentrated salts, reducing the complicating effect of particle aggregation, a problem that has been encountered in past applications of the

ACCEPTED MANUSCRIPT

technology [15]. By incorporating preparation methods previously developed for drug delivery [1], DNA-labeled particles were produced with diameters ranging from 60 nm to 1μm, allowing for the control of particle size to better match pathogens of interest, a benefit previously unavailable to studies utilizing this technology. This study also presents a clear and reliable relationship between particle concentration and DNA-label count which remains consistent across 7 orders of magnitude of particle concentration, a key component in illustrating the efficacy of this technology that has not yet been reported. Additionally, this study presents the results from environmental applications of the DNA-labeled particles, highlighting their ability to be used in environmental studies without interference between unique DNA-labels nor background biological media.

Whether exploring size-dependent transport phenomena or identifying potential pathogen transport pathways, a tool for the consistent identification of overlapping particle signals at a range of particle concentrations is crucial to success. Furthermore, the benefit of the DNA-labeled particles can be enhanced by also recovering the fraction retained on environmental surfaces. While early efforts of recovering the particles from soil has provided promising results [15], the process has not yet been refined. Ultimately, the utility of the DNA-labeled particle technology will be determined by how well it performs under varying conditions found in the natural environment (i.e. natural organic matter, pH, salinity), so the next step is to creatively apply the technology to help answer transport questions in the lab and environment.

5. Acknowledgements

This study was supported by the Heising-Simons Foundation (grant # 2014-59) and the University of California, Davis Department of Land, Air, and Water Resources. The authors would also like to acknowledge Professors Nitin Nitin and Tom Young for their aid in securing access to instrumentation crucial to this work as well as Dustin Flavell, Nikolas Schweitzer, Dr. Jeremy James, and all of the staff at the Sierra Foothills Research and Extension Center for consistent

ACCEPTED MANUSCRIPT

help and support.

ACCEPTED MANUSCRIPT

ACCEPTED MANUSCRIPT

References

[1] E. Sah, H. Sah, Recent trends in preparation of poly (lactide-co-glycolide) nanoparticles by mixing polymeric organic solution with antisolvent, Journal of Nanomaterials 16 (1) (2015) 61.

[2] R. Langer, New methods of drug delivery, Science (1990) 1527–1533.

[3] M. J. Alonso, Nanoparticulate drug carrier technology, Drugs and the pharmaceutical sciences 77 (1996) 203–242.

[4] F. Danhier, E. Ansorena, J. M. Silva, R. Coco, A. Le Breton, V. Préat, Plga-based nanoparticles: an overview of biomedical applications, Journal of controlled release 161 (2) (2012) 505–522.

[5] D. Luo, W. M. Saltzman, Synthetic DNA delivery systems, Nature biotechnology 18 (1) (2000) 33–37.

[6] K. Y. Win, S.-S. Feng, Effects of particle size and surface coating on cellular uptake of polymeric nanoparticles for oral delivery of anticancer drugs, Biomaterials 26 (15) (2005) 2713–2722.

[7] H. K. Makadia, S. J. Siegel, Poly lactic-co-glycolic acid (plga) as biodegradable controlled drug delivery carrier, Polymers 3 (3) (2011) 1377–1397.

[8] J. M. Chan, L. Zhang, K. P. Yuet, G. Liao, J.-W. Rhee, R. Langer, O. C. Farokhzad, Plga–lecithin–peg core–shell nanoparticles for controlled drug delivery, Biomaterials 30 (8) (2009) 1627–1634.

[9] A. Kumari, S. K. Yadav, S. C. Yadav, Biodegradable polymeric nanoparticles based drug delivery systems, Colloids and Surfaces B: Biointerfaces 75 (1) (2010) 1–18.

[10] J. Shaikh, D. Ankola, V. Beniwal, D. Singh, M. R. Kumar, Nanoparticle encapsulation improves oral bioavailability of curcumin by at least 9-fold when compared to curcumin administered with piperine as absorption enhancer, European Journal of Pharmaceutical Sciences 37 (3) (2009) 223–230.

ACCEPTED MANUSCRIPT

[11] L. R. Beck, D. R. Cowsar, D. H. Lewis, J. W. Gibson, C. E. Flowers, New long-acting injectable microcapsule contraceptive system, American journal of obstetrics and gynecology 135 (3) (1979) 419–426.

[12] J. M. Anderson, M. S. Shive, Biodegradation and biocompatibility of PLA and PLGA microspheres, Advanced drug delivery reviews 64 (2012) 72–82.

[13] A. N. Sharma, D. Luo, M. T. Walter, Hydrological tracers using nanobiotechnology: proof of concept, Environmental science & technology 46 (16) (2012) 8928–8936.

[14] H. E. Dahlke, A. G. Williamson, C. Georgakakos, S. Leung, A. N. Sharma, S. W. Lyon, M. T. Walter, Using concurrent dna tracer injections to infer glacial flow pathways, Hydrological Processes 29 (25) (2015) 5257–5274.

[15] C. Wang, C. P. McNew, S. W. Lyon, M. T. Walter, H. E. Dahlke, Particle tracer transport in a sloping soil lysimeter under periodic, steady state conditions, Manuscript submitted for publication.

[16] H. E. Dahlke, C. P. McNew, C. Wang, C. J. Harman, P. Troch, M. T. Walter, S. W. Lyon, Opening the doors of perception in hydrology with nanotechnology, Manuscript submitted for publication.

[17] X. Niu, W. Zou, C. Liu, N. Zhang, C. Fu, Modified nanoprecipitation method to fabricate DNA-loaded PLGA nanoparticles, Drug development and industrial pharmacy 35 (11) (2009) 1375–1383.

[18] S. Díez, C. T. de Ilarduya, Versatility of biodegradable poly (d, l-lactic-co-glycolic acid) microspheres for plasmid DNA delivery, European journal of pharmaceutics and biopharmaceutics 63 (2) (2006) 188–197.

[19] M. R. Kumar, U. Bakowsky, C. Lehr, Preparation and characterization of cationic PLGA nanospheres as DNA carriers, Biomaterials 25 (10) (2004) 1771–1777.

ACCEPTED MANUSCRIPT

[20] D. S. Knopman, C. I. Voss, S. P. Garabedian, Sampling design for groundwater solute transport: Tests of methods and analysis of cape cod tracer test data, Water Resources Research 27 (5) (1991) 925–949.

[21] P. R. Jørgensen, T. Helstrup, J. Urup, D. Seifert, Modeling of non-reactive solute transport in fractured clayey till during variable flow rate and time, Journal of Contaminant Hydrology 68 (3) (2004) 193–216.

[22] M. Dyck, R. Kachanoski, E. De Jong, Long-term movement of a chloride tracer under transient, semi-arid conditions, Soil Science Society of America Journal 67 (2) (2003) 471–477.

[23] L. K. Lautz, D. I. Siegel, R. L. Bauer, Impact of debris dams on hyporheic interaction along a semi-arid stream, Hydrological Processes 20 (1) (2006) 183–196.

[24] D. W. Metge, R. W. Harvey, R. Anders, D. O. Rosenberry, D. Seymour, J. Jasperse, Use of carboxylated microspheres to assess transport potential of cryptosporidium parvum oocysts at the russian river water supply facility, Sonoma County, California, Geomicrobiology Journal 24 (3-4) (2007) 231–245.

[25] L. Cathles, H. Spedden, E. Malouf, A tracer technique to measure the diffusional accessibility of matrix block mineralization, in: 103rd AIME annual meeting, The American Institute of Mining, Metallurgical, & Petroluem Engineers, Inc., Dallas, Texas, 1974, pp. 73–94005.

[26] J. E. Saiers, G. M. Hornberger, C. Harvey, Colloidal silica transport through structured, heterogeneous porous media, Journal of Hydrology 163 (3-4) (1994) 271–288.

[27] M. Flury, N. N. Wai, Dyes as tracers for vadose zone hydrology, Reviews of Geophysics 41 (1).

ACCEPTED MANUSCRIPT

[28] A. Heilig, T. S. Steenhuis, M. T. Walter, S. J. Herbert, Funneled flow mechanisms in layered soil: field investigations, Journal of Hydrology 279 (1) (2003) 210–223.

[29] H. E. Dahlke, S. W. Lyon, P. Jansson, T. Karlin, G. Rosqvist, Isotopic investigation of runoff generation in a glacierized catchment in northern sweden, Hydrological Processes 28 (3) (2014) 1383–1398.

[30] H. Wu, X. Zhang, L. Xiaoyan, G. Li, Y. Huang, Seasonal variations of deuterium and oxygen-18 isotopes and their response to moisture source for precipitation events in the subtropical monsoon region, Hydrological Processes 29 (1) (2015) 90–102.

[31] N. B. Basu, G. Destouni, J. W. Jawitz, S. E. Thompson, N. V. Loukinova, A. Darracq, S. Zanardo, M. Yaeger, M. Sivapalan, A. Rinaldo, et al., Nutrient loads exported from managed catchments reveal emergent biogeochemical stationarity, Geophysical Research Letters 37 (23).

[32] M. Kim, L. A. Pangle, C. Cardoso, M. Lora, T. H. Volkmann, Y. Wang, C. J. Harman, P. A. Troch, Transit time distributions and storage selection functions in a sloping soil lysimeter with time-varying flow paths: Direct observation of internal and external transport variability, Water Resources Research 52 (9) (2016) 7105–7129.

[33] C. A. Scott, M. F. Walter, G. N. Nagle, M. T. Walter, N. V. Sierra, E. S. Brooks, Residual phosphorus in runoff from successional forest on abandoned agricultural land: 1. biogeochemical and hydrological processes, Biogeochemistry 55 (3) (2001) 293–310.

[34] J. W. Kirchner, X. Feng, C. Neal, Fractal stream chemistry and its implications for contaminant transport in catchments, Nature 403 (6769) (2000) 524.

[35] B. J. Mahler, M. Winkler, P. Bennett, D. M. Hillis, Dna-labeled clay: a

ACCEPTED MANUSCRIPT

sensitive new method for tracing particle transport, Geology 26 (9) (1998) 831–834.

[36] I. H. Sabir, J. Torgersen, S. Haldorsen, P. Aleström, Dna tracers with information capacity and high detection sensitivity tested in groundwater studies, Hydrogeology Journal 7 (3) (1999) 264–272.

[37] H. Colleuille, N. O. Kitterod, Forurensning av drikkevannsbronn pa sundreoya i al kommune: Resultat av sportsoff-forsok, Norwegian Water Resources and Energy Directorate Report.

[38] G. Pietramellara, J. Ascher, F. Borgogni, M. Ceccherini, G. Guerri, P. Nannipieri, Extracellular dna in soil and sediment: fate and ecological relevance, Biology and Fertility of Soils 45 (3) (2009) 219–235.

[39] R. L. McCall, R. W. Sirianni, PLGA nanoparticles formed by single-or double-emulsion with vitamin E-TPGS, Journal of visualized experiments: JoVE (82).

[40] A. Kumar, K. K. Sawant, Application of multiple regression analysis in optimization of anastrozole-loaded plga nanoparticles, Journal of microencapsulation 31 (2) (2014) 105–114.

[41] Y.-C. Chen, W.-Y. Hsieh, W.-F. Lee, D.-T. Zeng, Effects of surface modification of plga-peg-plga nanoparticles on loperamide delivery efficiency across the blood–brain barrier, Journal of biomaterials applications 27 (7) (2013) 909–922.

[42] M. J. Santander-Ortega, N. Csaba, M. J. Alonso, J. L. Ortega-Vinuesa, D. Bastos-Gonzalez, Stability and physicochemical characteristics of plga, plga: poloxamer and plga: poloxamine blend nanoparticles: A comparative study, Colloids and Surfaces A: Physicochemical and Engineering Aspects 296 (1) (2007) 132–140.

[43] M. Santander-Ortega, A. Jódar-Reyes, N. Csaba, D. Bastos-González, J. Ortega-Vinuesa, Colloidal stability of pluronic f68-coated plga nanoparti-

ACCEPTED MANUSCRIPT

ACCEPTED MANUSCRIPT

cles: A variety of stabilisation mechanisms, Journal of colloid and interface science 302 (2) (2006) 522–529.

[44] S. M. Moghimi, A. C. Hunter, Poloxamers and poloxamines in nanoparticle engineering and experimental medicine, Trends in biotechnology 18 (10) (2000) 412–420.

[45] National Center for Biotechnology Information, Nucleotide primer-basic local alignment search tool (BLAST), `https://blast.ncbi.nlm.nih.gov/Blast.cgi`, accessed: 2017-07-27.

[46] L. Mu, S. Feng, A novel controlled release formulation for the anticancer drug paclitaxel (taxol®): Plga nanoparticles containing vitamin e tpgs, Journal of controlled release 86 (1) (2003) 33–48.

[47] S. Malathi, P. Nandhakumar, V. Pandiyan, T. J. Webster, S. Balasubramanian, Novel plga-based nanoparticles for the oral delivery of insulin, International journal of nanomedicine 10 (2015) 2207.

[48] T. Riley, T. Govender, S. Stolnik, C. Xiong, M. Garnett, L. Illum, S. Davis, Colloidal stability and drug incorporation aspects of micellar-like pla–peg nanoparticles, Colloids and surfaces B: Biointerfaces 16 (1) (1999) 147–159.

[49] S.-W. Choi, J.-H. Kim, Design of surface-modified poly (d, l-lactide-co-glycolide) nanoparticles for targeted drug delivery to bone, Journal of Controlled Release 122 (1) (2007) 24–30.

[50] K. Avgoustakis, A. Beletsi, Z. Panagi, P. Klepetsanis, E. Livaniou, G. Evangelatos, D. Ithakissios, Effect of copolymer composition on the physicochemical characteristics, in vitro stability, and biodistribution of plga–mpeg nanoparticles, International journal of pharmaceutics 259 (1) (2003) 115–127.

[51] S. A. Bradford, H. Kim, C. Shen, S. Sasidharan, J. Shang, Contributions of nanoscale roughness to anomalous colloid retention and stability behavior, Langmuir 33 (38) (2017) 10094–10105.

ACCEPTED MANUSCRIPT

[52] H. Cohen, R. Levy, J. Gao, I. Fishbein, V. Kousaev, S. Sosnowski, S. Slomkowski, G. Golomb, Sustained delivery and expression of dna encapsulated in polymeric nanoparticles, Gene therapy 7 (22) (2000) 1896.

[53] S. M. Abdelghany, D. J. Quinn, R. J. Ingram, B. F. Gilmore, R. F. Donnelly, C. C. Taggart, C. J. Scott, Gentamicin-loaded nanoparticles show improved antimicrobial effects towards pseudomonas aeruginosa infection, International journal of nanomedicine 7 (2012) 4053.

[54] C. Lecaroz, C. Gamazo, M. J. Renedo, M. J. Blanco-Prieto, Biodegradable micro-and nanoparticles as long-term delivery vehicles for gentamicin, Journal of microencapsulation 23 (7) (2006) 782–792.

[55] D. Cun, C. Foged, M. Yang, S. Frøkjær, H. M. Nielsen, Preparation and characterization of poly (dl-lactide-co-glycolide) nanoparticles for sirna delivery, International journal of pharmaceutics 390 (1) (2010) 70–75.

[56] Z. Zhang, S. Tongchusak, Y. Mizukami, Y. J. Kang, T. Ioji, M. Touma, B. Reinhold, D. B. Keskin, E. L. Reinherz, T. Sasada, Induction of antitumor cytotoxic t cell responses through plga-nanoparticle mediated antigen delivery, Biomaterials 32 (14) (2011) 3666–3678.

[57] S. Ribeiro, N. Hussain, A. T. Florence, Release of dna from dendriplexes encapsulated in plga nanoparticles, International journal of pharmaceutics 298 (2) (2005) 354–360.

[58] T. Musumeci, C. Bucolo, C. Carbone, R. Pignatello, F. Drago, G. Puglisi, Polymeric nanoparticles augment the ocular hypotensive effect of melatonin in rabbits, International journal of pharmaceutics 440 (2) (2013) 135–140.

[59] W.-P. Su, F.-Y. Cheng, D.-B. Shieh, C.-S. Yeh, W.-C. Su, Plga nanoparticles codeliver paclitaxel and stat3 sirna to overcome cellular resistance in lung cancer cells, International journal of nanomedicine 7 (2012) 4269.

ACCEPTED MANUSCRIPT

[60] Z. H. Wang, Z. Y. Wang, C. S. Sun, C. Y. Wang, T. Y. Jiang, S. L. Wang, Trimethylated chitosan-conjugated plga nanoparticles for the delivery of drugs to the brain, Biomaterials 31 (5) (2010) 908–915.

[61] H. Shen, X. Hu, M. Szymusiak, Z. J. Wang, Y. Liu, Orally administered nanocurcumin to attenuate morphine tolerance: comparison between negatively charged plga and partially and fully pegylated nanoparticles.

[62] L. Martín-Banderas, J. Álvarez-Fuentes, M. Durán-Lobato, J. Prados, C. Melguizo, M. Fernández-Arévalo, M. Á. Holgado, Cannabinoid derivate-loaded PLGA nanocarriers for oral administration: formulation, characterization, and cytotoxicity studies, International journal of nanomedicine 7 (2012) 5793.

[63] J. Ravindran, H. B. Nair, B. Sung, S. Prasad, R. R. Tekmal, B. B. Aggarwal, Thymoquinone poly (lactide-co-glycolide) nanoparticles exhibit enhanced anti-proliferative, anti-inflammatory, and chemosensitization potential, Biochemical pharmacology 79 (11) (2010) 1640.

[64] W. Bao, J. Zhou, J. Luo, D. Wu, Plga microspheres with high drug loading and high encapsulation efficiency prepared by a novel solvent evaporation technique, Journal of microencapsulation 23 (5) (2006) 471–479.

[65] A. Swarowsky, R. Dahlgren, A. O'Geen, Linking subsurface lateral flowpath activity with streamflow characteristics in a semiarid headwater catchment, Soil Science Society of America Journal 76 (2) (2012) 532–547.

[66] M. Elimelech, J. Gregory, X. Jia, Particle deposition and aggregation: measurement, modelling and simulation, Butterworth-Heinemann, 2013.

ACCEPTED MANUSCRIPT

ACCEPTED MANUSCRIPT

Appendix A. Particle Preparation Details

Bare PLGA particles were prepared following a method similar to those previously reported [43, 42, 1] and briefly described as follows. First, 50 mg PLGA was dissolved in 2 mL dichloromethane (DCM) overnight. Then, 0.2 mL ultrapure DI water was added and thoroughly mixed via vortex for 30 seconds. This step is to simulate inclusion of DNA labels (though none are included in this case) in order to remain consistent with the procedure for producing DNA-labeled particles. The resulting mixture is then slowly poured into a beaker of 25 mL ethanol, under moderate magnetic stirring, instantly resulting in a two-phase emulsion. 25 mL ultrapure DI water was then slowly added to the stirring emulsion and then allowed to stir for an additional 10 minutes. Finally, the DCM and ethanol were removed under vacuum at 30 ^{o}C (Buchi Rotovapor R110) and the resulting PLGA particle suspension was stored at 2 ^{o}C for the entirety of the study.

ACCEPTED MANUSCRIPT

ACCEPTED MANUSCRIPT

Appendix B. DNA sequences

Table B.1: Nucleotide sequences of the 4 DNA-labels, primers, and probes used in this study. Bold and underlined segments indicate forward and reverse primer locations.

T3	5'- AA**A GTA AAG CAG CAG AGG TGG ACA** GAG GAA GAG CAG AAG AAG GAA AGA ATG CTG GGA AGA GG**A AGA ACG CAA GGC AAA GCG GA**G GTA - 3'
T3 Probe	5'- /56-FAM/AGC AGA AGA /ZEN/AGG AAA GAA TGC TGG GA/3IABkFQ/ - 3'
T4	5'- AC**A CGG ATC AAT CGG ATG TCA GGA TTC** CCA GCT CGC AAC TTA CCG ACC TGG ATG AGG AGT GGC CGT GAA AG**C ACA GAC ACC GTA GAA AAG ACA ACC** CT - 3'
T4 Probe	5'- /5HEX/CGC AAC TTA /ZEN/CCG ACC TGG ATG AGG /3IABkFQ/ -3'
T10	5' - G**GC TCT CAC TGT GTA CAT GTG TTA T**CT GCC TTT CGT CGG GGC GGT AAT TCT TGG TGC ACA GA**C AAT CTT AAT AAG AGT CAG GAC TGG GT**C - 3'
T12	5'- C**CG TAG AGA TCT CCC ATC TGT CCT TTG** CTG AAG GTT AAA ACC CCG GAC CGC CTA GAA TAT TC**T TTC TTT AGC TCC AAA ATG GCC TCT** C - 3'

Appendix C. Additional Characterization Details

An aliquot of particle suspension was mixed with a pre-measured amount of mono (NaCl) or divalent ($CaCl_2$) salt and the mean particle diameter was immediately monitored over time. In this manner, the particle aggregation rate, or rate of change in particle diameter over time, k, was measured under varying ionic conditions. In each experiment, the particle concentration was held constant at 10 mg/L (2.8×10^4 particles/μL) and the solution was buffered to a pH of 7 using TE (5 mM Tris, 0.5 mM EDTA). The presence of ions in

ACCEPTED MANUSCRIPT

solution screens the electrical double layer repulsions between particles [66] and reduces the energy barrier to particle aggregation. This charge screening effect increases with ionic strength, until a salt concentration is reached where there is effectively no energy barrier to aggregation and therefore particle aggregation is only limited by the rate at which particles can diffuse towards one another. This concentration is known as the critical coagulation concentration (CCC) and by normalizing the aggregation rate under each condition to this diffusion limited aggregation rate (k_{diff}), we can calculate the inverse stability factor (Eq. C.1), which allows for the quantification of the stability of a particle suspension.

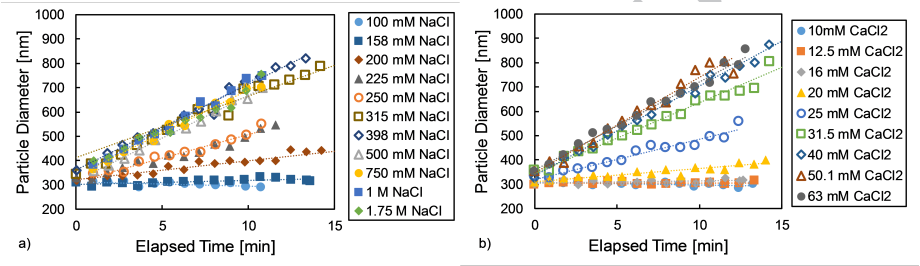

Figure C.11: Bare PLGA particle aggregation as a function of (a) NaCl and (b) $CaCl_2$ concentration.

$$\frac{1}{W} = \frac{k}{k_{diff}} \tag{C.1}$$

As expected, aggregation rate increased with salt concentration for the bare PLGA particles (Figure C.11) with an increased sensitivity to the presence of divalent $CaCl_2$. Initial aggregation rates were constant throughout all salt concentrations investigated, and so the first 10 minutes of particle aggregation were used to calculate the aggregation rate (k) for each condition investigated. The diffusion limited aggregation rate (k_{diff}) was taken to be the aggregation rate at which an increase in salt concentration did not result in an increase in aggregation rate. In this manner, the inverse stability factor ($1/W$) was determined for each experimental condition, as defined in Equation C.1, and

ACCEPTED MANUSCRIPT

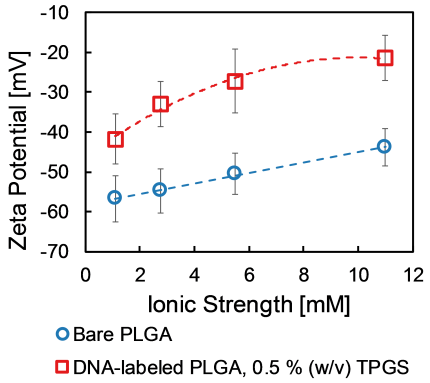

Figure C.12: Zeta potential of bare PLGA and DNA-labeled particles as a function of ionic strength. Error bars represent standard deviation. Experiments took place at pH 7 and particle concentration of 10 mg/L (2.8×10^4 particles/μL).

presented in Figure 5.

Displayed on a log-log scale, there are two distinct regions evident in the particle stability results presented in Figure 5. Within the first region, $1/W$ increases with salt concentration until the CCC is reached, after which $1/W$ remains constant at a value of 1. The CCC is then determined by interpolating the data to find the point where these two regions meet. In this manner, we determined the CCC values of bare PLGA particles to be 273 mM NaCl and 30 mM $CaCl_2$, which are similar to values reported in the literature [42, 43].

ACCEPTED MANUSCRIPT

Appendix D. Tabulated Data

Table D.2: Tabulated data contained in Figure 4.

pH	Bare PLGA μ_e 10^8 [m^2/Vs]	St. Dev.	DNA-labeled PLGA (0.50% TPGS) μ_e 10^8 [m^2/Vs]	St. Dev.
2.6	-0.28	0.50	-0.06	0.48
3.1	-0.79	0.40	-0.17	0.41
3.75	-1.53	0.41	-0.31	0.43
5.2	-2.40	0.50	-0.75	0.36
6.1	-3.33	0.46	-1.40	0.39
7.0	-3.43	0.63	-1.40	0.39
7.5	-3.50	0.45	-1.71	0.47
9.0	-3.90	0.50	-1.876	0.48

Table D.3: Tabulated data contained in Figure C.11.

NaCl Concentration [mM]	1/W	St. Dev.	$CaCl_2$ Concentration [mM]	1/W	St. Dev.
158	0.060	0.007	12.5	0.003	0.002
200	0.228	0.013	16	0.018	0.007
225	0.448	0.026	20	0.124	0.003
250	0.537	0.027	25	0.417	0.006
315	0.908	0.008	32	0.793	0.008
398	0.983	0.007	40	1.000	0.014
500	0.991	0.048	50	1.137	0.012
750	0.986	0.019	63	0.965	0.016
1000	1.006	0.028	-	-	-

ACCEPTED MANUSCRIPT

Table D.4: Tabulated data contained in Figure 7.

Particle Preparation Method	Encapsulation Efficiency [%]	St. Dev.	Extraction Efficiency [%]	St. Dev.
0.05% TPGS Double Emulsion	90.1	0.7	96.3	1.8
0.10% TPGS Double Emulsion	88.1	3.8	92.1	4.9
0.30% TPGS Double Emulsion	79.7	3.6	97.9	1.4
0.50% TPGS Double Emulsion	88.3	1.9	103.5	6.8
Indirect Nanoprecipitation	82.3	3.5	93.1	1.9
Direct Nanoprecipitation	82.2	4.2	91.1	5.2

ACCEPTED MANUSCRIPT

ACCEPTED MANUSCRIPT

Table D.5: Tabulated data contained in Figure 8.

Mass Concentration [mg/L]	Number Concentration [particles/μL]	DNA-Label Count [copies/μL]
9.94E+03	2.77E+07	3.26E+07
9.94E+03	2.77E+07	3.15E+07
9.94E+03	2.77E+07	3.15E+07
3.16E+03	8.80E+06	1.01E+07
3.16E+03	8.80E+06	1.10E+07
3.16E+03	8.80E+06	1.16E+07
9.99E+02	2.78E+06	4.51E+06
9.99E+02	2.78E+06	4.43E+06
9.99E+02	2.78E+06	4.48E+06
3.16E+02	8.79E+05	1.13E+06
3.16E+02	8.79E+05	1.09E+06
3.16E+02	8.79E+05	1.17E+06
9.98E+01	2.78E+05	4.25E+05
9.98E+01	2.78E+05	4.32E+05
9.98E+01	2.78E+05	4.17E+05
3.15E+01	8.78E+04	6.98E+04
3.15E+01	8.78E+04	6.65E+04
3.15E+01	8.78E+04	6.55E+04
9.96E+00	2.77E+04	2.36E+04
9.96E+00	2.77E+04	2.04E+04
9.96E+00	2.77E+04	2.21E+04
3.15E+00	8.76E+03	4.91E+03
3.15E+00	8.76E+03	3.85E+03
3.15E+00	8.76E+03	3.33E+03
9.95E-01	2.77E+03	1.98E+03
9.95E-01	2.77E+03	1.84E+03
9.94E-02	2.77E+02	4.21E+02

ACCEPTED MANUSCRIPT

Table D.6: Tabulated data contained in Figure 8, continued.

Mass Concentration [mg/L]	Number Concentration [particles/μL]	DNA-Label Count [copies/μL]
9.94E-02	2.77E+02	4.23E+02
3.14E-02	8.74E+01	6.97E+01
3.14E-02	8.74E+01	2.73E+01
9.92E-03	2.76E+01	2.23E+01
9.92E-03	2.76E+01	1.92E+01
1.05E+04	2.91E+07	6.53E+07
1.05E+04	2.91E+07	6.08E+07
1.05E+04	2.91E+07	6.04E+07
3.16E+03	8.80E+06	2.29E+07
3.16E+03	8.80E+06	2.17E+07
3.16E+03	8.80E+06	2.29E+07
9.99E+02	2.78E+06	4.19E+06
9.99E+02	2.78E+06	4.05E+06
9.99E+02	2.78E+06	4.08E+06
9.98E+01	2.78E+05	2.59E+05
9.98E+01	2.78E+05	2.59E+05
9.98E+01	2.78E+05	2.40E+05
3.15E+00	8.76E+03	5.50E+03
3.15E+00	8.76E+03	4.42E+03
3.15E+00	8.76E+03	4.10E+03
9.95E-01	2.77E+03	3.43E+03
9.95E-01	2.77E+03	3.63E+03
9.95E-01	2.77E+03	3.77E+03
3.14E-01	8.75E+02	4.99E+02
3.14E-01	8.75E+02	4.47E+02
3.14E-01	8.75E+02	4.63E+02
3.14E-02	8.74E+01	1.20E+02

ACCEPTED MANUSCRIPT

Table D.7: Tabulated data contained in Figure 8, continued.

Mass Concentration [mg/L]	Number Concentration [particles/μL]	DNA-Label Count [copies/μL]
3.14E-02	8.74E+01	8.48E+01
3.14E-02	8.74E+01	1.10E+02
9.92E-03	2.76E+01	3.59E+01
9.92E-03	2.76E+01	3.12E+01
9.92E-03	2.76E+01	4.79E+01
1.00E+03	2.78E+06	1.98E+06
1.00E+03	2.78E+06	1.88E+06
1.00E+03	2.78E+06	2.22E+06
9.94E-02	2.77E+02	1.39E+02

ACCEPTED MANUSCRIPT

Table D.8: Tabulated data contained in Figure 6.

Elapsed Time [min]	0.05% TPGS Particle Diameter [nm]	Elapsed Time [min]	0.10% TPGS Particle Diameter [nm]	Elapsed Time [min]	Nanoprecipitation Indirect Particle Diameter [nm]
0.00	1411	0.00	714	0.00	195
0.88	1369	0.90	689	0.88	209
1.78	1213	1.77	697	1.78	202
2.68	1253	2.67	729	2.67	198
3.57	1208	3.53	695	3.55	199
4.45	1126	4.42	730	4.43	206
5.35	1155	5.32	697	5.33	211
6.25	1222	6.20	644	6.22	204
7.15	1119	7.08	724	7.12	202
10.72	1294	7.97	722	8.00	195
11.62	1231	8.85	809	8.90	199
12.50	1166	9.75	727	9.80	201
13.40	1158	10.63	761	10.70	202
14.30	1077	11.52	745	11.58	203
-	-	12.40	705	12.48	201
-	-	13.28	709	13.37	199
-	-	14.18	704	14.27	197

ACCEPTED MANUSCRIPT

ACCEPTED MANUSCRIPT

Table D.9: Particle size, zeta potential, standard deviation, and polydispersity index of particles produced following each method presented in Figure 3.

Particle Preparation Method	Mean Particle Diameter [nm]	St. Deviation of Particle Diameter [nm]	Polydispersity Index (PDI)	Mean Zeta Potential [mV]	St. Deviation of Zeta Potential [mV]
Double Emulsion Method 0.05% TPGS	931	130	0.56	-43	6
Double Emulsion Method 0.10% TPGS	609	153	0.21	-41	6
Double Emulsion Method 0.30% TPGS	317	121	0.09	-40	6
Double Emulsion Method 0.50% TPGS	281	74	0.07	-42	6
Nanoprecipitation Method Indirect	108	35	0.10	-44	9
Nanoprecipitation Method Direct	59	50	0.28	-44	8

ACCEPTED MANUSCRIPT

ACCEPTED MANUSCRIPT

ACCEPTED MANUSCRIPT

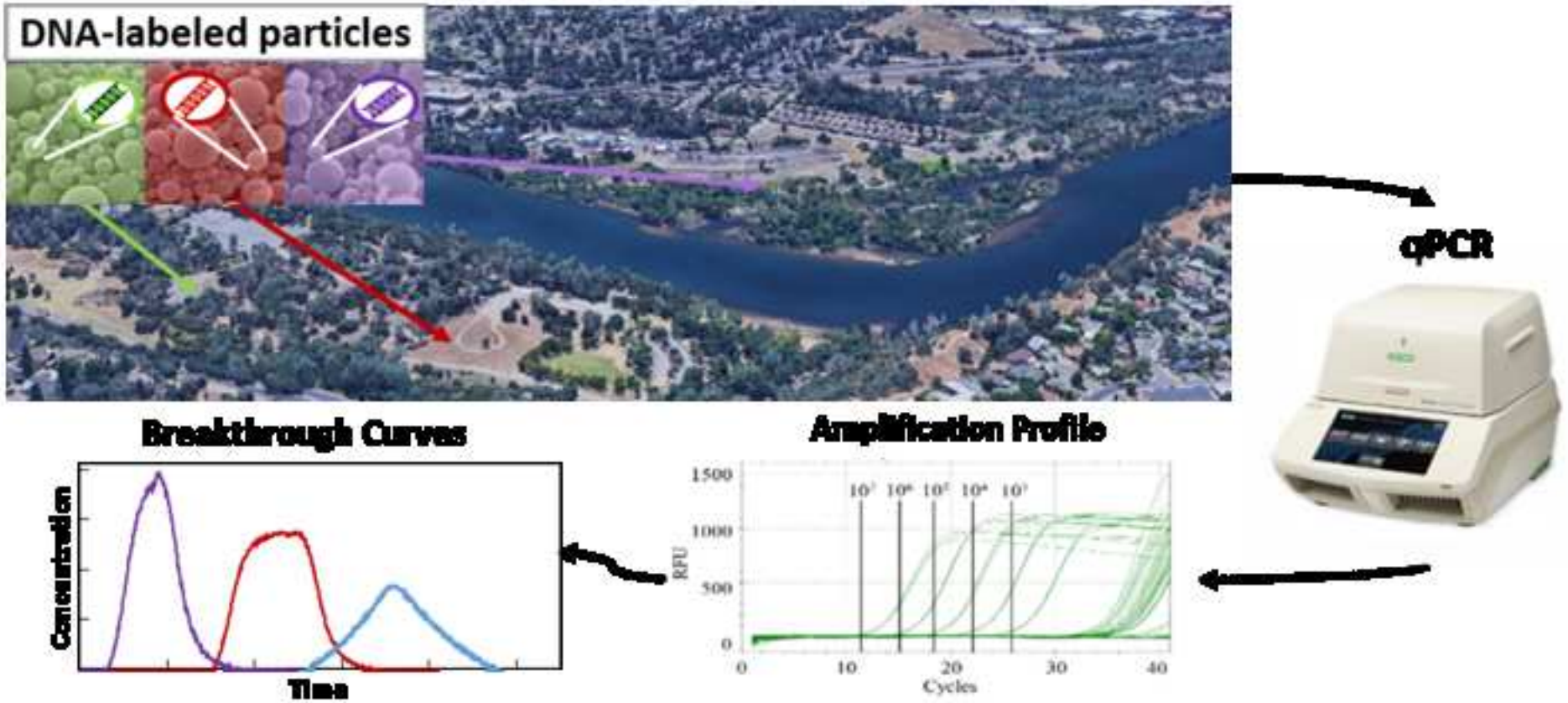

ACCEPTED